

Nondipole modification of the ac Stark effect in above-threshold ionizationSimon Brennecke and Manfred Lein ^{*}*Leibniz Universität Hannover, Institut für Theoretische Physik, Appelstraße 2, 30167 Hannover, Germany*

(Received 29 May 2021; accepted 2 August 2021; published 27 August 2021)

Above-threshold ionization (ATI) of atoms in intense laser pulses produces photoelectron momentum distributions that exhibit discrete concentric circles related to the absorption of more photons than required to exceed the ionization threshold. Using numerical solutions of the one-electron time-dependent Schrödinger equation beyond the electric dipole approximation for circularly polarized laser pulses, we show that the geometric centers of ATI rings are counterintuitively shifted against the propagation direction of the light, i.e., in the direction opposite to the on-average transferred photon momentum. From a comparison with a simple model based on energy considerations, we identify a nondipole modification of the ac Stark effect for electron continuum states as the origin of our observation.

DOI: [10.1103/PhysRevA.104.L021104](https://doi.org/10.1103/PhysRevA.104.L021104)

When an electronic system is placed in a static external electric field, the dc Stark effect shifts its energy levels. Similarly, the influence of an oscillating external electromagnetic field modifies the electronic structure, known as the dynamical or ac Stark effect. This ac Stark effect results in a plethora of observations reaching from the Autler-Townes effect [1] to the Mollow triplet in resonance fluorescence [2,3] to nonresonant phenomena in intense laser pulses, such as the alignment of molecules [4], the shaping of potential energy surfaces [5], or the time-dependent modification of propagating laser pulses [6,7]. Mathematically, the dynamical Stark effect can be described in Floquet theory [8,9] by introducing “dressed” quasienergy states.

In intense visible or infrared laser pulses, multiphoton ionization can occur by absorption of more photons than required to exceed the ionization threshold [10]. Hence, in above-threshold ionization (ATI), the photoelectron energy distributions show peaks separated by the photon energy ω and the photoelectron momentum distributions consist of rings corresponding to the various numbers of absorbed photons (atomic units are used unless stated otherwise). In such strong ultrafast laser pulses, the dynamical Stark effect shifts the energies of the continuum states as well as highly excited states of atoms approximately by the ponderomotive potential U_p that can reach several tens of electron volts. For a field with peak field strength E_0 , frequency ω , and ellipticity ϵ ($0 \leq \epsilon \leq 1$), the ponderomotive potential is $U_p = \frac{E_0^2}{4\omega^2}(1 + \epsilon^2)$. In contrast, tightly bound ground states are typically only weakly affected by the Stark shift. As a result, in direct nonresonant ionization as it occurs in circularly polarized fields, the positions of the ATI rings are modified by the continuum ac Stark effect [11,12]. Using a simple energy argument, the ATI peak positions for ionization in multicycle subpicosecond

laser pulses are usually estimated as [12]

$$n\omega = I_p + \frac{\mathbf{p}^2}{2} + U_p \quad (1)$$

with the final electron momentum \mathbf{p} , the field-free ionization potential I_p , and n being an integer that can be interpreted as the number of absorbed photons [13]. In linearly polarized fields, Stark-shifted bound-state resonances (Freeman resonances) lead to a rich additional substructure of the ATI rings at low energies [14].

ATI is usually discussed in the electric dipole approximation, where only the temporal evolution of the electric field is considered and the magnetic field is completely neglected. As a result, the momentum distributions of the emitted electrons from atoms are forward-backward symmetric and the ATI rings are centered at momentum $\mathbf{p} = 0$ [see Eq. (1)]. Here, “forward” denotes the laser propagation direction (z direction). For the laser parameters used in most tabletop experiments, the nondipole corrections are small. However, in recent experiments, the transfer of photon momentum to the photoelectrons and, hence, the breaking of the forward-backward symmetry have been observed [15–20]. The experimental findings have been supported by theoretical investigations based on the numerical solution of the time-dependent Schrödinger equation (TDSE) [21–24], approximate theories based on the strong-field approximation (SFA) [25–29], or the semiclassical approximation [16,30–32]. For recollision-free ionization, e.g., in circularly polarized fields, the overall momentum distribution is slightly shifted in the light-propagation direction such that the average momentum component in the light-propagation direction is positive [18,25–27]. The major part of the forward shift is directly proportional to the kinetic energy E_e gained due to the acceleration in the laser field. Intuitively speaking, the forward shift is a consequence of radiation pressure.

The above-quoted works on nondipole effects in strong-field ionization focus either on the modification of the envelope of the probability distribution, typically represented

^{*}lein@itp.uni-hannover.de

by the average momentum component in light propagation direction, or on rescattering phenomena. Even though the appearance of ATI peaks is a prominent manifestation of multiphoton light-matter interaction, the nondipole modification of the ATI peak geometry has been only addressed in various SFA-type approaches [33–35]. Here, we close this gap by solving the TDSE for circularly polarized laser pulses and by showing that the geometric structure of the ATI rings is modified by nondipole effects; i.e., the ATI rings are not lines of constant kinetic energy anymore. Interestingly, we find that the centers of the ATI rings are shifted against the light propagation direction and, hence, in the direction opposite to the on-average transferred photon momentum. We demonstrate that this is a signature of a nondipole modification of the ac Stark effect for continuum electrons.

In order to calculate photoelectron momentum distributions (PMDs) beyond the electric dipole approximation, we consider the TDSE in a single-active-electron approximation for a plane-wave light pulse with electrodynamic potentials $\phi(\mathbf{r}, t) = 0$ and $\mathbf{A}(\mathbf{r}, t) = \mathbf{A}(t - z/c)$. We follow the scheme presented in Refs. [18,24]; i.e., the theory covers the dynamics within magnetic dipole and electric quadrupole approximations. Here, the time evolution is governed by the Hamiltonian

$$H = \frac{1}{2} \left[\mathbf{p} + \mathbf{A}(t) + \frac{\mathbf{e}_z}{c} \left(\mathbf{p} \cdot \mathbf{A}(t) + \frac{1}{2} \mathbf{A}^2(t) \right) \right]^2 + V \left(\mathbf{r} - \frac{z}{c} \mathbf{A}(t) \right), \quad (2)$$

where the vector potential $\mathbf{A}(\eta)$ is related to the electric field by $\mathbf{E}(\eta) = -\partial_\eta \mathbf{A}(\eta)$. The TDSE is solved numerically using the split-operator method with a time step of $\Delta t = 0.03$ a.u. on a Cartesian grid with 1024 points in each dimension and a spacing of $\Delta x = 0.4$ a.u. To obtain the momentum distribution, outgoing parts of the wave function are projected onto nondipole Volkov states via an absorber [36] that starts at a distance of 160 a.u. from the center, which provides accurate results according to our convergence checks. The momentum distribution is only calculated for a slice in the p_x - p_z plane at $p_y = 0$ with a resolution of $\Delta p_x = \Delta p_z = 0.0019$ a.u. The atomic binding potential for a helium atom is chosen as in Tong and Lin [37] with the singularity removed by using a pseudopotential for the $1s$ state (with a cutoff radius of $r_{\text{cl}} = 1.5$ a.u.) [38]. In order to suppress Freeman resonances, we consider direct ionization in circularly polarized laser pulses defined by the vector potential $\mathbf{A}(\eta)$ with either a \sin^2 envelope of 14 cycles duration or a trapezoidal pulse shape, where the field is switched on and off using linear ramps of two cycles duration and in between its intensity is constant for 5.5 cycles duration.

For circularly polarized multicycle laser pulses, the PMDs have a donutlike shape, i.e., they are approximately rotationally symmetric in the polarization plane (here the p_x - p_y plane). Hence, in Fig. 1 we only show a slice through the momentum distribution for ionization of helium by a trapezoidal laser pulse with 800 nm wavelength and an intensity of 4×10^{14} W/cm². The distribution consists of ATI rings that are sections of concentric circles. When calculated within the dipole approximation, the PMDs are symmetric with respect to the polarization plane. However, nondipole contributions

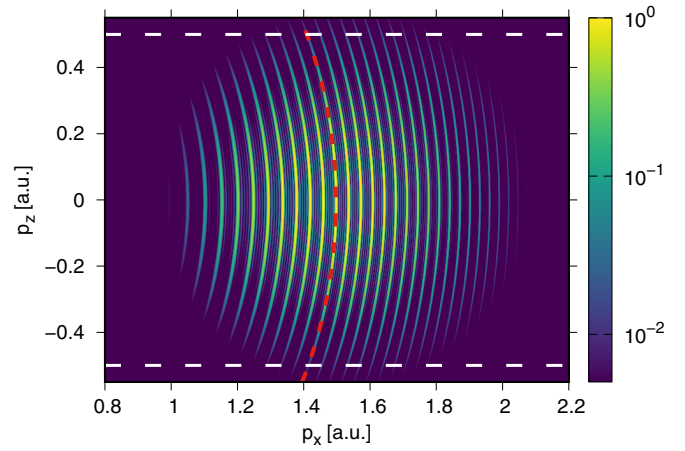


FIG. 1. Two-dimensional slice through the photoelectron momentum distribution at $p_y = 0$ for ionization of helium by a trapezoidal laser pulse with a wavelength of 800 nm and an intensity of 4×10^{14} W/cm². The red dashed line indicates the position $p_x(p_z)$ of one selected ATI ring.

lead to a symmetry breaking of the PMDs in the light propagation direction (the z direction). To observe these small effects more clearly, we show in Fig. 2(a) one-dimensional slices through the distribution at $p_z = \pm 0.5$ a.u. as a function of p_x (see the white dashed lines in Fig. 1). In agreement with earlier works, the probability in the forward direction is higher than that in the backward direction. This overall forward shift of the envelope of the momentum distribution results in the positive expectation value $\langle p_z \rangle \approx 0.0104$ a.u. of the momentum component in the light propagation direction. Already in a pioneering work, Smeenk *et al.* [15] have experimentally shown that the average value $\langle p_z \rangle$ is approximately given by the prediction $\langle E_e \rangle / c$, with $\langle E_e \rangle$ being the kinetic energy gained due to the laser field. Later, it was theoretically proposed that there is an additional forward shift of about $I_p / (3c)$ [25,26] which has recently been experimentally confirmed [18].

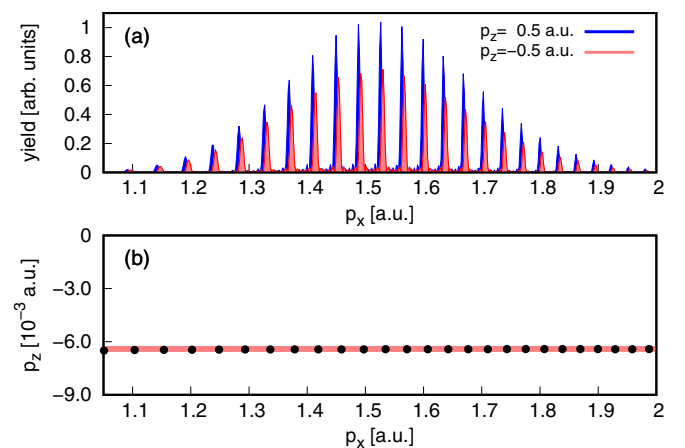


FIG. 2. (a) One-dimensional slices at $p_z = \pm 0.5$ a.u. through the distribution of Fig. 1. (b) Shift p_z^{ATI} of the ATI ring against the light propagation direction for the different ATI rings plotted as a function of $p_x(p_z^{\text{ATI}})$. The thick red line shows the simple estimate of Eq. (8).

Additionally, we find that the positions of the ATI peaks are also different in forward and backward directions [see Fig. 2(a)]. This means that the ATI rings are not lines of constant kinetic electron energy anymore. To further study this effect, we determine the position $p_x(p_z)$ as a function of p_z for each ring. The result for one selected ring is shown as a red dashed line in Fig. 1. The maximum of $p_x(p_z)$ and, hence, the center of the ATI ring are not located at $p_z = 0$, but are shifted slightly backwards to negative values $p_z^{\text{ATI}} \approx -0.0064$ a.u. It is surprising that the positions of the ATI rings are displaced in the opposite direction compared to the average value $\langle p_z \rangle$; i.e., the ATI substructure is shifted opposite to the envelope of the momentum distribution. We find that all analyzed ATI rings, regardless of the number of absorbed photons, are approximately centered at the same position [see Fig. 2(b)].

In order to explore the origin of the ATI peak shift, we consider the quasienergy levels of the atom in a periodic electromagnetic plane-wave field. Using Floquet theory and treating the electromagnetic field classically, the tightly bound ground state is driven well below any resonant frequencies (for wavelengths in the visible or infrared) and, hence, the quasienergy is approximately given by the negative field-free ionization potential $-I_p$. In contrast, the continuum states experience large ac Stark shifts. To estimate the nondipole contributions to the quasienergies, we may consider the nondipole Volkov states that are solutions of the potential-free TDSE [39,40]. As described in Ref. [41], the states can be expressed as (to first order in $1/c$)

$$|\psi_{\mathbf{p}}^{\text{V}}(t)\rangle = e^{-iS(\mathbf{p},t)}|\mathbf{p}\rangle, \quad (3)$$

consisting of plane waves $|\mathbf{p}\rangle$ and the generalized action

$$S(\mathbf{p}, t) = \frac{1}{2} \int^t d\zeta \mathbf{v}^2(\mathbf{p}, \zeta), \quad (4)$$

with

$$\mathbf{v}(\mathbf{p}, t) = \mathbf{p} + \mathbf{A}(t) + \frac{\mathbf{e}_z}{c} \left(\mathbf{p} \cdot \mathbf{A}(t) + \frac{1}{2} \mathbf{A}^2(t) \right). \quad (5)$$

For a T -periodic field with $\mathbf{A}(t) = \mathbf{A}(t + T)$, the nondipole Volkov states are directly related to the time-periodic Floquet states $|\theta_{\mathbf{p}}^{\text{F}}(t)\rangle = |\psi_{\mathbf{p}}^{\text{V}}(t)\rangle e^{iE_{\text{F}}t}$. Here, the quasienergy of a state with momentum \mathbf{p} is given in first order of $1/c$ by

$$E_{\text{F}} = \frac{\mathbf{p}^2}{2} + \left(1 + \frac{p_z}{c} \right) U_p, \quad (6)$$

with the well-known ponderomotive potential $U_p = \frac{1}{T} \int_0^T d\eta \frac{1}{2} \mathbf{A}^2(\eta)$. For sufficiently short pulses (typically in the subpicosecond range), the photoelectrons stay in the interaction region throughout the pulse and, thus, electrons in a Floquet state with the momentum label \mathbf{p} will be detected with the final momentum \mathbf{p} after the laser field is switched off. Therefore, Eq. (6) can be interpreted as the laser-modified energy (ac-Stark-shifted energy) of a continuum state. The ac Stark shift of the continuum states can be read off as $(1 + \frac{p_z}{c})U_p$. As in the dipole approximation, all continuum states are shifted up in energy. However, electrons that travel in the light propagation direction ($p_z > 0$) are shifted to energies slightly higher than those of electrons that are traveling against the direction of the light wave ($p_z < 0$).

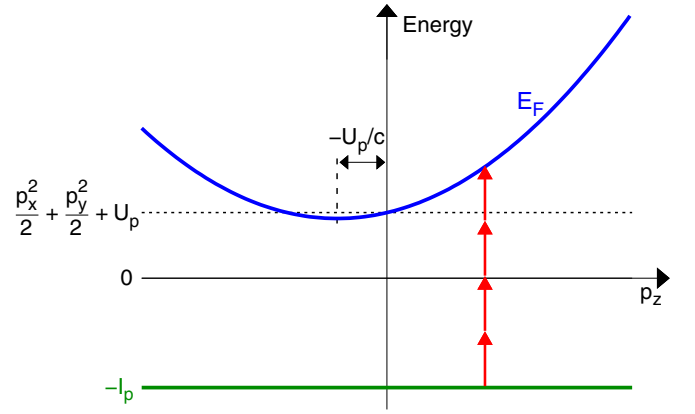


FIG. 3. Schematic illustration of the ac-Stark-shifted quasienergies (with an exaggerated value of $1/c$). The blue line shows the quasienergies, Eq. (6), of the potential-free continuum states as a function of the p_z -momentum component in the light propagation direction for fixed $p_x^2 + p_y^2$. If a continuum state with a given momentum $p_z > 0$ can be reached by absorption of n photons, then the continuum state with $-p_z$ and the same $p_x^2 + p_y^2$ cannot be reached by absorption of the same number of photons.

Starting from the ground state with energy $-I_p$, the energy conservation dictates which continuum states may be populated by absorption of n photons:

$$n\omega = I_p + \frac{\mathbf{p}^2}{2} + \left(1 + \frac{p_z}{c} \right) U_p. \quad (7)$$

Hence, if a continuum state with momentum component $p_z > 0$ may be reached by absorbing n photons, the continuum state with momentum component $-p_z$ (but same $p_x^2 + p_y^2$) cannot be reached by absorption of the same number of photons due to the different ac Stark shifts. The situation is schematically sketched in Fig. 3. This explains the different positions of the ATI peaks in Fig. 2(a). Furthermore, the energy conservation of Eq. (7) implies that the ATI peaks are still circles in the final momentum space. However, the centers of the rings are uniformly shifted towards slightly negative p_z momenta:

$$p_z^{\text{ATI}} = -\frac{U_p}{c} < 0. \quad (8)$$

We find that the simple estimate of Eq. (8) is in excellent agreement with the numerical solution of the TDSE [see Fig. 2(b)].

In addition to the energy-based explanation presented above, the appearance of ATI peaks can also be described in the time domain. Here, the interference between contributions ejected in each period of the laser field leads to interference maxima. In the strong-field approximation [25–29], the phase difference for electrons released in two consecutive periods of the laser fields is given by

$$\Delta\varphi = S(\mathbf{p}, t + T) - S(\mathbf{p}, t) + I_p T, \quad (9)$$

with the action S of Eq. (4). The condition for constructive interference, $\Delta\varphi = 2\pi n$ with $n \in \mathbb{Z}$, defines the positions of the maxima in the momentum distribution. Using the periodicity of the laser fields, this condition simplifies (to first order in $1/c$) to the energy conservation of Eq. (7). In the SFA,

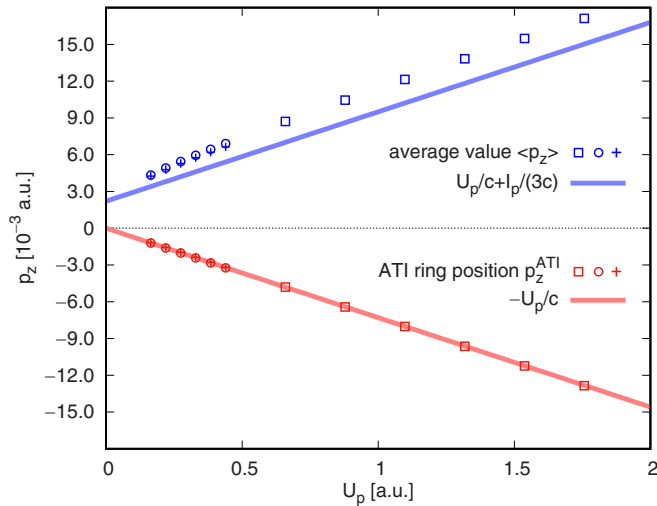


FIG. 4. Shift of the ATI ring position p_z^{ATI} and expectation value $\langle p_z \rangle$ of the momentum in light propagation as a function of the ponderomotive potential U_p , extracted from PMDs obtained by numerical solution of the TDSE for various laser parameters: Trapezoidal pulses with 800 nm wavelength (squares), trapezoidal pulses with 400 nm wavelength (circles), and pulses with \sin^2 envelope and 400 nm wavelength (crosses). The intensities are in the range between 3×10^{14} and 8×10^{14} W/cm 2 . The red line indicates the simple estimate for the ATI peak position of Eq. (8) and the blue line indicates the simple estimate for the average momentum $\langle p_z \rangle \approx \frac{U_p}{c} + \frac{I_p}{3c}$ in circularly polarized fields [15,18,25,26].

the condition has already been found in Refs. [33–35], but it has neither been discussed in detail nor verified by numerical simulations.

As the ponderomotive potential U_p depends strongly on the laser’s intensity and wavelength, the simple estimate of Eq. (8) predicts also a strong variation of the nondipole shift of the ATI peaks with the laser parameters. To study this

influence, we determine PMDs for intensities ranging from 3×10^{14} to 8×10^{14} W/cm 2 and two different wavelengths of 800 and 400 nm using a trapezoidal laser pulse. In addition, for 400 nm, we repeat the calculations for a more realistic \sin^2 -laser pulse of 14 cycles duration, where contributions to the ionization signal from the leading and falling edges of the pulse with smaller intensities are more pronounced. In all cases, we find a linear scaling of the ATI ring positions with the ponderomotive potential U_p (see Fig. 4). The TDSE results are in excellent agreement with the estimate of Eq. (8). For all studied laser parameters, the comparison with the expectation value $\langle p_z \rangle$ of the momentum in light propagation shows that the shifts of the ATI ring positions are in the same order as, but opposite to, the shift of the envelope of the PMD.

In conclusion, we have analyzed the ATI peak structure beyond the electric dipole approximation. We have found that the ATI rings are displaced in the direction opposite to the propagation direction of the radiation and, hence, also opposite to the shift of the envelope of the momentum distribution. Microscopically, the ATI peak shift can be explained by a nondipole modification of the ac Stark effect for continuum states. The ac Stark shift is larger for electrons that travel with the light wave than for electrons that travel antiparallel to the light. This leads to a simple model, which is in excellent agreement with the numerical solution of the TDSE for circular polarization. Since this model does not rely on the used laser polarization, we believe that the ATI peak shift will also be present for other wave forms as long as nonresonant ionization dominates. However, if Stark-shifted bound-state resonances are present, e.g., in linearly polarized fields [14] or two-color circularly polarized fields [42], we expect that interesting, more complex nondipole modifications of the ATI peaks will occur.

We thank Reinhard Dörner and Sebastian Eckart for fruitful discussions. S.B. thanks the German Academic Exchange Service (DAAD) for financial support.

-
- [1] S. H. Autler and C. H. Townes, Stark effect in rapidly varying fields, *Phys. Rev.* **100**, 703 (1955).
 - [2] B. R. Mollow, Power spectrum of light scattered by two-level systems, *Phys. Rev.* **188**, 1969 (1969).
 - [3] J. Dalibard and C. Cohen-Tannoudji, Laser cooling below the Doppler limit by polarization gradients: Simple theoretical models, *J. Opt. Soc. Am. B* **6**, 2023 (1989).
 - [4] H. Stapelfeldt and T. Seideman, Colloquium: Aligning molecules with strong laser pulses, *Rev. Mod. Phys.* **75**, 543 (2003).
 - [5] B. J. Sussman, D. Townsend, M. Yu. Ivanov, and A. Stolow, Dynamic Stark control of photochemical processes, *Science* **314**, 278 (2006).
 - [6] V. Kalosha, M. Spanner, J. Herrmann, and M. Ivanov, Generation of Single Dispersion Precompensated 1-fs Pulses by Shaped-Pulse Optimized High-Order Stimulated Raman Scattering, *Phys. Rev. Lett.* **88**, 103901 (2002).
 - [7] P. J. Bustard, B. J. Sussman, and I. A. Walmsley, Amplification of Impulsively Excited Molecular Rotational Coherence, *Phys. Rev. Lett.* **104**, 193902 (2010).
 - [8] J. H. Shirley, Solution of the Schrödinger equation with a Hamiltonian periodic in time, *Phys. Rev.* **138**, B979 (1965).
 - [9] H. Sambe, Steady states and quasienergies of a quantum-mechanical system in an oscillating field, *Phys. Rev. A* **7**, 2203 (1973).
 - [10] P. Agostini, F. Fabre, G. Mainfray, G. Petite, and N. K. Rahman, Free-Free Transitions Following Six-Photon Ionization of Xenon Atoms, *Phys. Rev. Lett.* **42**, 1127 (1979).
 - [11] P. H. Bucksbaum, R. R. Freeman, M. Bashkansky, and T. J. McIlrath, Role of the ponderomotive potential in above-threshold ionization, *J. Opt. Soc. Am. B* **4**, 760 (1987).
 - [12] P. H. Bucksbaum, L. D. Van Woerkom, R. R. Freeman, and D. W. Schumacher, Nonresonant above-threshold ionization by

- circularly polarized subpicosecond pulses, *Phys. Rev. A* **41**, 4119 (1990).
- [13] A. Szöke, Interpretation of electron spectra obtained from multiphoton ionisation of atoms in strong fields, *J. Phys. B* **18**, L427 (1985).
- [14] R. R. Freeman, P. H. Bucksbaum, H. Milchberg, S. Darack, D. Schumacher, and M. E. Geusic, Above-Threshold Ionization with Subpicosecond Laser Pulses, *Phys. Rev. Lett.* **59**, 1092 (1987).
- [15] C. T. L. Smeenk, L. Arissian, B. Zhou, A. Mysyrowicz, D. M. Villeneuve, A. Staudte, and P. B. Corkum, Partitioning of the Linear Photon Momentum in Multiphoton Ionization, *Phys. Rev. Lett.* **106**, 193002 (2011).
- [16] A. Ludwig, J. Maurer, B. W. Mayer, C. R. Phillips, L. Gallmann, and U. Keller, Breakdown of the Dipole Approximation in Strong-Field Ionization, *Phys. Rev. Lett.* **113**, 243001 (2014).
- [17] J. Maurer, B. Willenberg, J. Daněk, B. W. Mayer, C. R. Phillips, L. Gallmann, M. Klaiber, K. Z. Hatsagortsyan, C. H. Keitel, and U. Keller, Probing the ionization wave packet and recollision dynamics with an elliptically polarized strong laser field in the nondipole regime, *Phys. Rev. A* **97**, 013404 (2018).
- [18] A. Hartung, S. Eckart, S. Brennecke, J. Rist, D. Trabert, K. Fehre, M. Richter, H. Sann, S. Zeller, K. Henrichs, G. Kastirke, J. Hoehl, A. Kalinin, M. S. Schöffler, T. Jahnke, L. Ph. H. Schmidt, M. Lein, M. Kunitski, and R. Dörner, Magnetic fields alter strong-field ionization, *Nat. Phys.* **15**, 1222 (2019).
- [19] B. Willenberg, J. Maurer, B. W. Mayer, and U. Keller, Sub-cycle time resolution of multi-photon momentum transfer in strong-field ionization, *Nat. Commun.* **10**, 5548 (2019).
- [20] A. Hartung, S. Brennecke, K. Lin, D. Trabert, K. Fehre, J. Rist, M. S. Schöffler, T. Jahnke, L. Ph. H. Schmidt, M. Kunitski, M. Lein, R. Dörner, and S. Eckart, Electric Nondipole Effect in Strong-Field Ionization, *Phys. Rev. Lett.* **126**, 053202 (2021).
- [21] S. Chelkowski, A. D. Bandrauk, and P. B. Corkum, Photon-momentum transfer in multiphoton ionization and in time-resolved holography with photoelectrons, *Phys. Rev. A* **92**, 051401(R) (2015).
- [22] I. A. Ivanov, J. Dubau, and K. T. Kim, Nondipole effects in strong-field ionization, *Phys. Rev. A* **94**, 033405 (2016).
- [23] S. Chelkowski, A. D. Bandrauk, and P. B. Corkum, Photon-momentum transfer in photoionization: From few photons to many, *Phys. Rev. A* **95**, 053402 (2017).
- [24] S. Brennecke and M. Lein, High-order above-threshold ionization beyond the electric dipole approximation, *J. Phys. B* **51**, 094005 (2018).
- [25] S. Chelkowski, A. D. Bandrauk, and P. B. Corkum, Photon Momentum Sharing between an Electron and an Ion in Photoionization: From One-Photon (Photoelectric Effect) to Multiphoton Absorption, *Phys. Rev. Lett.* **113**, 263005 (2014).
- [26] M. Klaiber, E. Yakaboylu, H. Bauke, K. Z. Hatsagortsyan, and C. H. Keitel, Under-the-Barrier Dynamics in Laser-Induced Relativistic Tunneling, *Phys. Rev. Lett.* **110**, 153004 (2013).
- [27] P. L. He, D. Lao, and F. He, Strong Field Theories beyond Dipole Approximations in Nonrelativistic Regimes, *Phys. Rev. Lett.* **118**, 163203 (2017).
- [28] A. S. Titi and G. W. F. Drake, Quantum theory of longitudinal momentum transfer in above-threshold ionization, *Phys. Rev. A* **85**, 041404(R) (2012).
- [29] H. R. Reiss, Relativistic effects in nonrelativistic ionization, *Phys. Rev. A* **87**, 033421 (2013).
- [30] Th. Keil and D. Bauer, Coulomb-corrected strong-field quantum trajectories beyond dipole approximation, *J. Phys. B* **50**, 194002 (2017).
- [31] J. Daněk, M. Klaiber, K. Z. Hatsagortsyan, C. H. Keitel, B. Willenberg, J. Maurer, B. W. Mayer, C. R. Phillips, L. Gallmann, and U. Keller, Interplay between Coulomb-focusing and non-dipole effects in strong-field ionization with elliptical polarization, *J. Phys. B* **51**, 114001 (2018).
- [32] S. Brennecke and M. Lein, Strong-field photoelectron holography beyond the electric dipole approximation: A semiclassical analysis, *Phys. Rev. A* **100**, 023413 (2019).
- [33] H. R. Reiss, Relativistic strong-field photoionization, *J. Opt. Soc. Am. B* **7**, 574 (1990).
- [34] B. Böning, W. Paufler, and S. Fritzsche, Nondipole strong-field approximation for spatially structured laser fields, *Phys. Rev. A* **99**, 053404 (2019).
- [35] S. V. B. Jensen, M. M. Lund, and L. B. Madsen, Nondipole strong-field-approximation Hamiltonian, *Phys. Rev. A* **101**, 043408 (2020).
- [36] M. Lein, J. P. Marangos, and P. L. Knight, Electron diffraction in above-threshold ionization of molecules, *Phys. Rev. A* **66**, 051404(R) (2002).
- [37] X. M. Tong and C. D. Lin, Empirical formula for static field ionization rates of atoms and molecules by lasers in the barrier-suppression regime, *J. Phys. B* **38**, 2593 (2005).
- [38] N. Troullier and J. L. Martins, Efficient pseudopotentials for plane-wave calculations, *Phys. Rev. B* **43**, 1993 (1991).
- [39] M. W. Walser, C. H. Keitel, A. Scrinzi, and T. Brabec, High Harmonic Generation Beyond the Electric Dipole Approximation, *Phys. Rev. Lett.* **85**, 5082 (2000).
- [40] C. C. Chirilă, N. J. Kylstra, R. M. Potvliege, and C. J. Joachain, Nondipole effects in photon emission by laser-driven ions, *Phys. Rev. A* **66**, 063411 (2002).
- [41] S. Brennecke and M. Lein, High-order above-threshold ionization beyond the electric dipole approximation: Dependence on the atomic and molecular structure, *Phys. Rev. A* **98**, 063414 (2018).
- [42] P. Stammer, S. Patchkovskii, and F. Morales, Evidence of ac-Stark-shifted resonances in intense two-color circularly polarized laser fields, *Phys. Rev. A* **101**, 033405 (2020).